This article has been accepted for publication in a future issue of this journal, but has not been fully edited. Content may change prior to final publication. Citation information: DOI 10.1109/TPWRD.2015.2478709, IEEE Transactions on Power Delivery

Adaptive Power System for Managing Large Dynamic Loads

Deanna Temkin, Tyler Boehmer, and Amy Billups

***Abstract*—The Navy's future and near-term high-energy sensors and energy weapons will consume a large portion of the resources of the intended ship platform. Many of these new systems will have extreme dynamic power profiles, including both periodic and aperiodic characteristics. These dynamics can cause sudden changes in power at the prime power system that can be stressing to platform systems, both to the generators and prime movers as well as other loads sharing the common distribution bus. This paper presents the use of a new Adaptive Power System (APS) to mitigate the negative impacts levied on the platforms resulting from large dynamic loads. A notional size of the hardware required to implement the APS design is presented along with simulation results verifying the concept.**

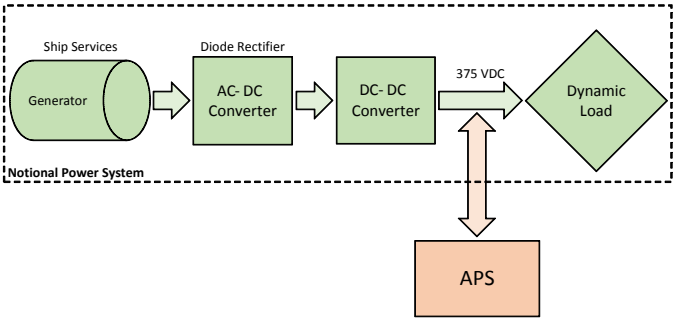

Fig. 1. A block diagram of a notional power system with the APS attached.

I. Introduction

THE Navy's future and near-term high-energy sensors and energy weapons present a challenge to the existing shipboard gensets and power distribution systems. These systems not only require higher power levels than seen in the past, but also have more extreme dynamic profiles. The profiles can range from periodic and predictable to aperiodic and unpredictable. Duty cycles can vary from small to continuous and, for some cases, the peak power demands can be above the capability of the ship power plant. These types of extreme power profiles cannot be supported with conventional power systems.

A block diagram of a conventional shipboard power system is shown in the dashed box of Figure 1. Conventional systems have focused heavily on providing well-regulated voltages and clean power to the corresponding load. If the voltage dynamics seen at the load are to be minimized, the output impedance of each converter stage is minimized by using small series inductance values, large shunt capacitance values, and control loops with high bandwidths. However, this type of system does little to prevent the mid to low frequency load dynamics from propagating back to the distribution bus and generator.

If the dynamic profiles propagate back to the ship's electric plant, significant power quality issues and generator/distribution losses can occur [1], [2]. In addition, the dynamic pulse loading may cause wear and tear on the gensets' mechanical parts [3]–[5]. Torsional stresses to the shaft of the ship's prime mover can result due to the very large and quickly changing electromagnetic load torques. These dynamic electromagnetic load torques may also excite the shaft's torsional resonances, typically referred to as sub-synchronous resonances [2], [6], adding additional stresses to the shaft.

Present-day methods that can be used to buffer the prime power system from dynamic loads include the following:

1) The **"brute-force method"**, whereby passive filters are used to smooth the dynamics of the load profile. Although this method results in minimal additional power losses, achieving the smoothing or filtering needed by the shipboard power system requires filter sizes and weights that are impractical and prohibitive for ship installation.
2) The **"throw-away-power method"**, whereby when the load is not using the maximum power allocated, the excess power is dissipated in an active load [7]. This type of system maintains a constant load profile to the generators, thus addressing the genset reliability and bus disturbance concerns. However, it can have severe impacts on system efficiency resulting from the large additional power dissipation, increasing both cooling requirements and fueling costs for ship platforms.
3) The **"restricted-timeline method"**, which requires a defined charging time for the system whereby the pulse power can only be supplied at predefined scheduled time intervals. For these systems, the successive launch times or fire times (repetition rate) and corresponding system performance are limited by the charging times of the system. Some examples of such systems are the Electromagnetic Aircraft Launch System (EMALS) and rail guns [8], [9].

Consequently, a new approach is needed to manage the load dynamics of emerging Navy systems – one that is not compromised by the disadvantages noted above for existing systems. The new Adaptive Power System (APS) specifically addresses this need. The APS can be used to efficiently mitigate bus disturbances and reduce stress to the shipboard gensets by converting the dynamic power load seen by the shipboard power system into an equivalent rolling time average – essentially serving as an active low pass filter to the load

This article has been accepted for publication in a future issue of this journal, but has not been fully edited. Content may change prior to final publication. Citation information: DOI 10.1109/TPWRD.2015.2478709, IEEE Transactions on Power Delivery

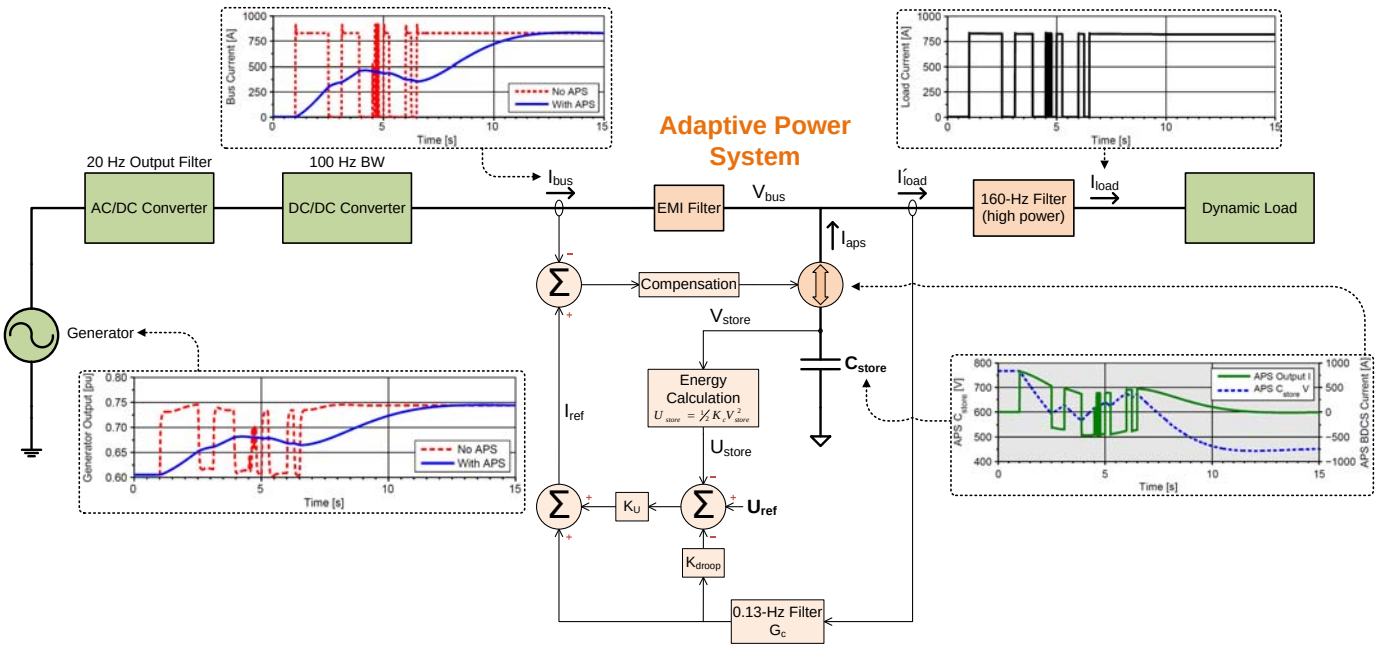

Fig. 2. An overview of the functionality of the APS system.

dynamics. As shown in Figure 1, the APS can be added to an existing system. The APS consists of energy storage, a passive power filter, a bi-directional current source, and innovative control loops, as shown in Figure 2. The bi-directional current source efficiently delivers the pulsed power demand from the APS energy storage to the desired sensor or weapon system, thus providing a buffer to the upstream power equipment.

The APS can support the pulsed load at a fraction of the size and weight needed when compared with the passive filter method (brute-force method), without excessive power dissipation as would exist if using the active load method (throw-away method), and for some specific applications without timeline restrictions as would be needed if using a refresh or recharging type system (restricted-timeline method).

If for all of the desired combinations for duty cycle, repetition rate, and peak power levels, the average power over a load cycle is within the allotted generator power, the APS can be designed such that no timeline restrictions exist. This is the case for the example of the 300-kW system given in Section III.

On the other hand, if there are profiles whereby the average power is above the generator capability, the APS can be used to provide the needed delta in power, allowing this enhanced operation of the sensor/weapon for short periods of time. The time limit for the enhanced operation is limited by the APS size, the size of the energy storage needed to provide the delta power, and the maximum average power allowed. This maximum allowed average power determines the corresponding duty cycle of this enhanced operation and hence the quickest allowed recharge time of the APS energy storage.

The APS is similar to the active filter concept whereby the active filter provides the current needed to maintain the quality of the load current required by the upstream power system. Active filters have been used for years in alternating current (AC) power systems to reduce the current harmonics and improve the power factor presented to the source when the loads are nonlinear and electrically noisy [10]–[12]. In addition, active filters have recently become popular in direct current (DC) systems to reduce conducted emissions caused by the pulse width modulation (PWM) switching action of the DC/DC converter load [13]. For an AC system the active filter produces a corresponding output current that when combined with the load current results in a clean sinusoidal current at the power system's fundamental frequency (e.g., 60 Hz). For a DC system the active filter operation is very similar to that for an AC system with the high frequency PWM switching noise of the load being canceled. Typical use of the active filter has focused on removing the harmonic currents (or for DC systems, the PWM switching currents and corresponding harmonics) riding on top of the average power draw. These noise current magnitudes are usually much less than the fundamental or DC current magnitude.

Conversely, for the new sensors and weapons it is not just a matter of removing a small level of noise riding on top of the average power draw. For these types of loads, the average power draw is not constant and may vary greatly. In addition, these dynamic loads not only produce noise at harmonic frequencies but also large levels of noise at inter-harmonic (not multiples of 60 Hz) and sub-harmonic (less than 60 Hz) frequencies. With the proper use of control loops and energy storage, the APS can reduce the rate at which the power demand on the generator changes, thus limiting the dynamics and spectral content seen by the generator - transforming a weapon or sensor system that had otherwise been incompatible with the platform's power system into one that is now feasible.

Section II proposes a requirement for the APS that considers the generator and prime-mover capabilities and limitations.

This article has been accepted for publication in a future issue of this journal, but has not been fully edited. Content may change prior to final publication. Citation information: DOI 10.1109/TPWRD.2015.2478709, IEEE Transactions on Power Delivery

Section III provides the operational overview and the detailed design for the APS to support a 300-kW dynamic load. Closed-form equations for sizing the energy storage are also provided in this section along with the needed transfer function for optimizing and controlling the system. In addition, Section III provides full system simulations (combined generator/APS/load) of this 300-kW notional configuration demonstrating significant improvement in generator voltage and frequency deviations during a large load disturbance when using the APS.

II. Proposed Requirements

The Navy's MIL-STD-1399-680 addresses pulse loading requirements, but only deals with pulses that occur infrequently – less than once every 45 seconds [14]. A requirement is needed that protects the genset and distribution bus against the dynamics resulting from frequent and repetitive pulsing loads but which is not as restrictive as the present requirement of only allowing a single pulse once every 45 seconds. Meeting the following requirement would provide this protection, and with the use of the APS, this requirement is feasible to implement, even for systems with large dynamic power profiles.

- **Proposed Pulsed Load Requirement**: The combined three-phase peak power ripple as seen by the shipboard generator(s) at any single frequency generated by the load shall be less than the limits defined by Figure 3.

The resulting allowed load profile proposed in Figure 3 has been matched to the generator and prime mover performance. Typical gensets' response times to a significant load change are on the order of 1.0 to 1.5 sec [15], [16]. If the rise and fall times for power changes (ramp rate) seen by the generator are controlled to be slower than the genset's response times, the generator and prime-mover control loops will be able to maintain the voltage and speed regulation, bus disturbances will be kept to a minimum for such a slow-changing power profile, and sub-synchronous resonances will not be excited because the disturbances are at lower frequencies than the shaft resonances. Additional losses and bus disturbances due to high harmonic and inter-harmonic noise will also be eliminated. The 3% value for frequencies greater than 1 Hz is chosen in order to be consistent with the existing 60 Hz harmonic line current requirement specified in MIL-STD-1399-680.

III. Adaptive Power System (APS)

A. Overview

The goal of the APS is to minimize bus disturbances and stress to prime-power equipment by converting the dynamic power load into an equivalent rolling average of the power demand. The APS is designed to meet the proposed requirement as shown in Figure 3. In addition, the APS implementation must also not interfere with maintaining a stiff voltage (tightly regulated voltage) to the load.

The top-level components of the APS include the energy storage capacitance and two control loops. One loop controls the APS output current to provide the required dynamic current to the load using the energy from the storage capacitance, and the other loop maintains the voltage across the energy storage capacitance to within the allowed rating.

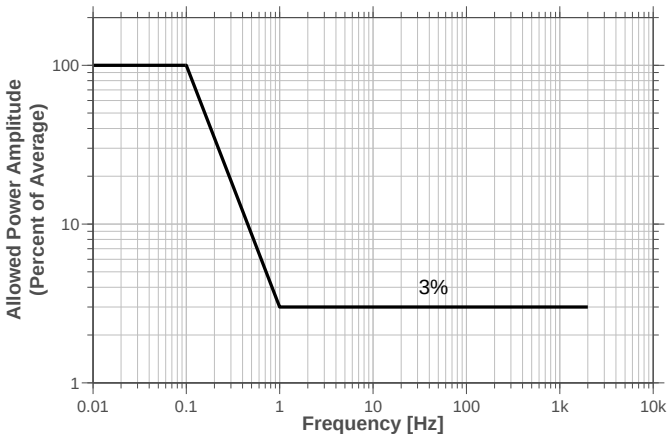

Fig. 3. The power ripple filtering requirement of the APS.

Figure 2 provides the detail voltage and current waveforms for the APS as well as the generator power waveform during the application of a dynamic load profile. Operation of the Adaptive Power System is as follows:

- The current provided from the upstream power system is regulated by the APS to be equal to the filtered (0.13 Hz) current profile of the load demand. The compensation block regulates I_{bus} to be equal to I_{ref} by controlling the output current of the bi-directional current source (BDCS); see the bus-current and BDCS-current waveforms in Figure 2. The BDCS is a DC/DC converter that can process power in both directions – it can both absorb and deliver power.
- Hence, the AC component or dynamics of the load profile is not part of I_{bus} but is provided by the energy-storage capacitance via the BDCS.
- The energy-storage capacitance value is selected to be large enough to provide the source and sink currents to support the pulsed load demand. The value for the energy-storage capacitance is minimized by allowing the voltage across C_{store} to vary significantly, where $U_{delivered} = \frac{1}{2}C_{store}(V_{t0}^2 - V_{t+}^2)$, minimizing the energy-storage capacitance required.
  - This provides significant weight and size savings compared to using an in-line high-powered low- pass filter (brute-force method).
  - The voltage variation across C_{store} is also decoupled from the load, allowing tight regulation of the bus voltage seen by the load to be maintained.

  $U_{delivered}$ is the energy delivered or absorbed by the storage capacitance, and V_{t0} and V_{t+} are the corresponding voltages across the energy-storage capacitance just prior to the load disturbance and after the energy-storage capacitance has delivered or absorbed the desired energy.
- The current reference, I_{ref}, is slowly adjusted to keep the voltage across C_{store} within the allowable boundaries. This is achieved by regulating the energy stored in C_{store} via a slow-moving outer loop. The block labeled K_u in

This article has been accepted for publication in a future issue of this journal, but has not been fully edited. Content may change prior to final publication. Citation information: DOI 10.1109/TPWRD.2015.2478709, IEEE Transactions on Power Delivery

Figure 2 sets the bandwidth of the outer energy loop while K_{droop} is used to optimize the energy utilization of C_{store}.

Controlling the load dynamics is accomplished by properly selecting the corner frequency for the 0.13-Hz signal filter in the current feedback path to be lower than the genset's control loop bandwidths. The corner-frequency selection for the signal filter is the critical design parameter in the APS that controls the protection provided to the generator and prime mover; hence this filter sets the allowed power ramp rate and dynamics seen by the generator.

To limit the bandwidth requirement of the APS, a low-pass filter between the APS and the load is used. The low-pass filter reduces the response-time requirement on the APS by reducing the high-frequency components of the load pulses seen at the bus connection to the BDCS. The corner frequency for the low-pass filter shown in Figure 2 is approximately 160 Hz.

The APS can both sink and source current through the BDCS, which is implemented with an efficient high-frequency DC/DC converter. Because the pulsed power is no longer provided by the generator, the value of C_{store} must be selected large enough to provide the source and sink currents to support the pulsed load demand in the time consistent with the 0.13-Hz signal-filter time constant, while concurrently maintaining the voltage across C_{store} within its defined allowable range.

The voltage range on C_{store} is indirectly controlled by regulating the energy stored in C_{store}. The current command, I_{ref}, is slowly adjusted to maintain the proper energy storage, thus keeping the proper voltage range across C_{store}. Energy regulation is chosen over voltage regulation to linearize the outer loop transfer function with respect to the BDCS controlled output current. Energy regulation eliminates the outer-loop dependency on the duty cycle of the BDCS. The duty cycle of the BDCS varies with the voltage across C_{store}. Because the transfer function $\frac{U_{delivered}(s)}{I_{aps}(s)}$ is independent of the voltage across C_{store}, as desired the outer bandwidth will remain constant as the voltage across C_{store} changes. If a voltage loop is used instead, the outer-loop bandwidth will vary with the DC operating point, potentially affecting performance.

To reduce the energy-storage capacitance needed, an adaptive reference for the energy-storage loop is used, whereby the reference is biased by the 0.13-Hz filtered load current. This technique is very similar to droop compensation regulation. If the 0.13-Hz filtered load current is at the maximum value, then the reference for the energy storage will be set to the minimum value, putting the capacitor in the optimal state for absorbing energy. If the 0.13-Hz filtered load current is at zero Amps, then the reference for the energy storage will be set to the maximum value, putting the capacitor in the optimal state for providing energy. This adaptive control maximizes the energy storage utilization by reducing the required capacitance by a factor of 2.

B. APS Requirements for Notional System

To demonstrate the APS functionality and performance, a top-level design and simulation for a notional 300-kW system was performed. For this specific system the APS interfaces with the 375-VDC bus, as shown in Figure 1. The system was designed to support the following load and input–output performance specifications:

- Duty Cycle of Load: 0 to continuous
- Average Load Power: 0 to 300 kW
- Peak Load Power: 0 to 300 kW
- Input Voltage: 4160 VAC per MIL-STD-1399-680
- Input Interface Power Ripple Requirements: Figure 3
- Voltage Transients at the 375-V Bus Load Interface: maintain to better than $\pm 5\%$

C. APS Design Details for Notional System

This section highlights some of the more critical design details of the APS. Specifically, bandwidth considerations for the various control loops are provided along with the derivation of a closed-form equation for the transfer function of load current to bus current, $\frac{I_{bus}(s)}{I_{load}(s)}$, and the derivation of the equation for determination of C_{store} value. These two equations are central to the design of the APS. Part values for the main components are also given in Table I allowing for performance metrics such as sizing and power dissipation for the 300-kW notional system to be predicted as presented in Tables I and II.

Control Loop Bandwidth Considerations: Figure 6 provides the schematic details for the APS. The bi-directional current source is a modular design consisting of thirty-eight 8-kW modules. The sizing and performance for the BDCS is based on the bi-directional buck topology [17], using a 100-kHz switching frequency and average current-mode control. The switching frequency is chosen high enough to obtain the needed control loop bandwidths (which will give the desired APS filtering performance) but low enough to maintain acceptable switching losses. The inner current loop bandwidth of the bi-directional current source is set to be between 15 and 25 kHz (varies with the voltage across C_{store}), allowing the outer current loop of the APS to be set at 4 kHz.

The bandwidth for the energy outer control loop is set at 0.02 Hz. This bandwidth is chosen high enough to maintain the energy and voltage compliance on C_{store} but low enough to meet the current-ripple requirement. If the outer energy control loop had a high bandwidth, the desired reference command for current would be heavily weighted to tightly regulate the energy on the capacitor. This would distort the APS output current, and hence the APS would not provide the desired compensation for the dynamic load current.

Transfer Function $\frac{I_{bus}(s)}{I_{load}(s)}$ and C_{store}: To determine the necessary energy-storage bank size, closed-form equations for the transfer function $\frac{I_{bus}(s)}{I_{load}(s)}$ and C_{store} are necessary. Because the desired behavior of the APS at very low frequencies (less than 1 Hz) determines the required energy-storage capacitance, the current control loops with the high bandwidths (4 kHz and 15 kHz) can be assumed ideal for these derivations, which means that for low frequencies it can be assumed that the bus current follows the reference command (see I_{ref} in Figure 2). Further simplifications used in this derivation include the assumptions that the bus voltage is constant for

This article has been accepted for publication in a future issue of this journal, but has not been fully edited. Content may change prior to final publication. Citation information: DOI 10.1109/TPWRD.2015.2478709, IEEE Transactions on Power Delivery

low frequencies, that the energy transfer between C_{store} and the bus is lossless, i.e., the energy delivered or absorbed by the storage capacitance equals $V_{bus} \cdot I_{aps}$, and that the EMI filter and the 160-Hz filter also have no effect at the low frequencies of interest.

To determine the transfer function $\frac{I_{bus}(s)}{I_{load}(s)}$, the APS piece of the block diagram shown in Figure 2 was converted to an equivalent signal flow graph, as shown in Figure 4. To simplify the analysis, the preceding assumptions have been used, and therefore this signal flow graph is only valid for low frequencies.

In Figure 4, I_{bus} is the controlled upstream bus current coming from the 375-V converter, I_{load} is the current to the load before the 160-Hz filter, and G_c is the transfer function of the 0.13-Hz filter, which has been selected to be a second-order filter defined as

$$G_c = \frac{\omega_c^2}{s^2 + (2\zeta\omega_c)s + \omega_c^2}, \tag{1}$$

where ω_c is the corner frequency (in rad/s) and ζ is the damping ratio. In this example, ζ is equal to 0.9.

In addition, K_u is the energy-loop gain that determines the energy outer loop bandwidth, K_{droop} is the gain of the energy droop compensation (in J/A), C_{act} is the actual capacitance of C_{store} (in Farads), and K_c is the capacitance value (in Farads) used in converting the measured capacitor bank voltage, V_{store}, to energy, such that the calculated stored energy is $\frac{1}{2}K_c V_{store}^2$. Using digital control, K_c could be programmed based on C_{act} to optimize the APS response as C_{act} varies over the life of the system. Ideally, K_c equals C_{act} and $\frac{K_c}{C_{act}}$ would then equal 1.

Using the signal flow graph method, as defined in reference [18] along with Figure 4, the transfer function $\frac{I_{bus}(s)}{I_{load}(s)}$ can be determined as follows:

$$\frac{I_{bus}(s)}{I_{load}(s)} = \sum_{k=1}^{N} \frac{P_k \Delta_k}{\Delta}, \tag{2}$$

where N is the total number of forward paths, P_k is the gain of the k^{th} forward path, Δ is the determinant, and Δ_k is the cofactor of path k. The gain of forward paths are defined as

$$\begin{aligned} P_1 &= G_c, \\ P_2 &= -K_{droop} K_u G_c, \\ P_3 &= K_u \frac{K_c}{C_{act}} \frac{\overline{V_{bus}}}{s}, \end{aligned} \tag{3}$$

where the bar over V_{bus} indicates a constant average value. There is only one loop in Figure 4, which is defined as

$$L = -K_u \frac{K_c}{C_{act}} \frac{\overline{V_{bus}}}{s}. \tag{4}$$

The determinant is then

$$\Delta = 1 - L = 1 + K_u \frac{K_c}{C_{act}} \frac{\overline{V_{bus}}}{s}. \tag{5}$$

Because the loop, L, touches all the forward paths, the cofactor for each forward path is simplify defined by

$$\Delta_1 = \Delta_2 = \Delta_3 = 1. \tag{6}$$

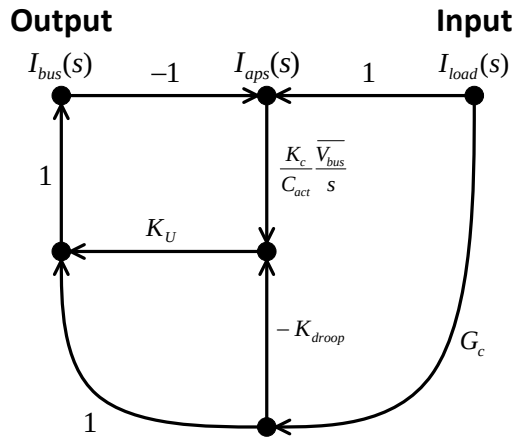

Fig. 4. Signal flow graph of APS for low frequency energy loop design where $I_{bus} = I_{ref}$ and $I_{load} = I'_{load}$.

This leads to a third-order model that includes just the 0.13-Hz filter characteristics and the energy-loop compensation characteristics, such that

$$\begin{aligned} \frac{I_{bus}(s)}{I_{load}(s)} &= \frac{P_1\Delta_1 + P_2\Delta_2 + P_3\Delta_3}{\Delta}, \\ &= \frac{G_c - K_{droop}K_u G_c + K_u \frac{K_c}{C_{act}} \frac{\overline{V_{bus}}}{s}}{1 + K_u \frac{K_c}{C_{act}} \frac{\overline{V_{bus}}}{s}}, \\ &= \frac{b_2 s^2 + b_1 s + b_0}{s^3 + a_2 s^2 + a_1 s + a_0}, \end{aligned}$$

$$\begin{aligned} \text{where } b_2 &= \frac{K_c}{C_{act}} \overline{V_{bus}} K_u, \\ b_1 &= \omega_c^2 - K_{droop} K_u \omega_c^2 + 2\frac{K_c}{C_{act}} \overline{V_{bus}} \zeta K_u \omega_c, \\ b_0 &= \frac{K_c}{C_{act}} \overline{V_{bus}} K_u \omega_c^2, \\ a_2 &= \frac{K_c}{C_{act}} \overline{V_{bus}} K_u + 2\zeta\omega_c, \\ a_1 &= \omega_c^2 + 2\frac{K_c}{C_{act}} \overline{V_{bus}} \zeta K_u \omega_c, \\ a_0 &= \frac{K_c}{C_{act}} \overline{V_{bus}} K_u \omega_c^2. \end{aligned} \tag{7}$$

To use equation (7), initially set K_{droop} equal to zero. Then set K_u to a value that will produce a curve for $\frac{I_{bus}(s)}{I_{load}(s)}$ that matches the requirement from 0.1 Hz to 1 Hz. Next, empirically set K_{droop} to the largest value possible whereby the requirement curve is still matched and the overshoot and undershoot of the transfer function are minimized. Notice in this equation that the K_{droop} term only shows up in the numerator coefficient b_1. Hence, K_{droop} only affects the damping ratio for the numerator. If the ratio $\frac{K_c}{C_{act}}$ is equal to one, the damping ratio for the numerator reduces to

$$\zeta_{num} = \frac{\omega_c}{2}\left(\frac{1}{\overline{V_{bus}} K_u} - \frac{K_{droop}}{\overline{V_{bus}}} + \frac{2\zeta}{\omega_c}\right). \tag{8}$$

Also note the sign in front of K_{droop} is negative, thus K_{droop}

This article has been accepted for publication in a future issue of this journal, but has not been fully edited. Content may change prior to final publication. Citation information: DOI 10.1109/TPWRD.2015.2478709, IEEE Transactions on Power Delivery

decreases the damping of the numerator. The value of K_{droop} should be such to produce a positive value for the numerator damping ratio. For large values of K_{droop} the numerator damping ratio will be negative, producing an undesirable response due to the resulting numerator right-half plane zeroes. Further fine tuning of the response can be performed by applying a step load to this transfer function $\frac{I_{bus}(s)}{I_{load}(s)}$ and making small adjustments to K_{droop} while observing the resulting waveform of I_{bus} in the time domain, with the goal being to achieve a critically-damped response. An overdamped response will increase the energy storage capacitance value. An underdamped response will cause overshoot in the response. In this example, K_{droop} equals 744.8 J/A and K_u equals 335e-6.

Figure 5 demonstrates that this equation's predictions (black dashed line) are nearly identical to the detailed simulation results (solid blue line) up to 4 Hz, at which point interactions with the current control-loop compensator begins to appear. This is sufficient to design the low-frequency characteristics of the APS response and to size the necessary capacitance for the energy-storage bank. Also shown in Figure 5 is the current-ripple rejection requirement (red dashed curve with the 100% and the 3% limits annotated) derived from the proposed power-ripple requirement in Figure 3 assuming the 375-V bus is a regulated bus. The red dashed curve represents both the allowed current ripple and the allowed power ripple when using the appropriate y-axis.

Figure 5 provides the time-constant requirement via the frequency-domain specification needed to determine the storage-capacitance nominal value, C_{design}. This requirement defines how long the APS needs to source the load current or sink the load current to provide sufficient protection to the generator and prime mover. This criteria is captured by the design parameter K_{droop}.

Hence, if K_u and K_{droop} have been selected as previously defined, where the requirements curve is met with a critically-damped response, the amount of energy used for a stepped load from fully off to fully on can be determined from K_{droop} and the maximum load current. This results since K_{droop}'s units are Joules/Ampere. Knowing the amount of energy used,

$$U_{total} = I_{loadmax} K_{droop}, \tag{9}$$

along with the maximum available energy for use,

$$U_{max} = \frac{1}{2} C_{design} (V_{max}^2 - V_{min}^2), \tag{10}$$

the corresponding capacitance value can be solved for

$$C_{design} = \frac{2 I_{loadmax} K_{droop}}{(V_{max}^2 - V_{min}^2)}. \tag{11}$$

Here, $I_{loadmax}$ is the designed maximum load current of the module, V_{max} is the maximum allowed capacitor voltage, V_{min} is the minimum allowed capacitor voltage.

This equation assumes that the energy reference in Figure 6 is set to the energy stored by the capacitance at the maximum voltage value, and that K_{droop}'s value is set to adjust this energy-reference level to the minimum value (minimum voltage across C_{store}) when the load current is at a maximum. For the notional design example, the maximum voltage is set at 770 V and the minimum voltage is set at 450 V. This gives a capacitance value needed per module of 86.7 mF for this thirty-eight-module system, resulting in a maximum stored energy per module equal to 25.7 kJ.

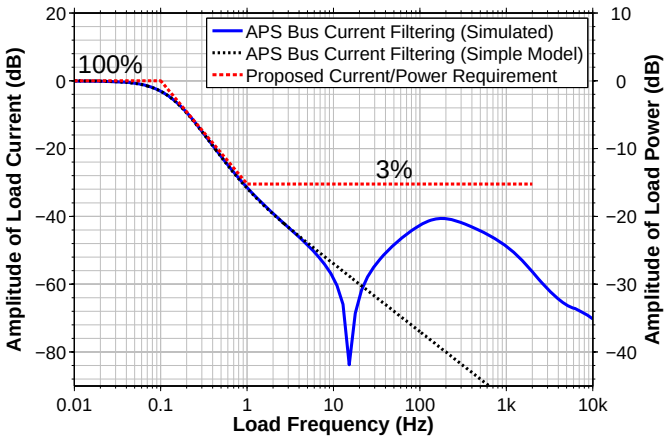

Fig. 5. The bus current filtering performance of the APS with the proposed requirement overlaid (for example, a 100 kW average load is allowed 3 kW peak ripple at 1 Hz). Because the bus voltage is approximately constant, current filtering directly relates to power filtering.

TABLE I
SIZE AND WEIGHT OF THE APS SYSTEM

Component	Value	Size (ft^3)	Weight (lbs.)
Module			
$L_{of} + R_{lof}$	10 μH + 1 mΩ	0.001	0.15
C_2*	3.3 μF	--	--
RC_2branch*	0.91 Ω + 68 μF	--	--
$L_{sw} + R_{sw}$	0.1 mH + 6 mΩ	0.004	1.4
C_{store}	86.7 mF	2.1	169.2
Heat Sinks	-	0.1	4
Miscellaneous	-	0.1	10
Total Modules			38
EMI Filter			
$L_1 + R_1$	25 μH + 0.3 mΩ	0.12	49
C_1	94 μF	0.01	1
RC_1branch	0.31 Ω + 1.9 mF	0.03	5
Low-Pass Filter			
$L_f + R_{fs}$	25 μH + 0.3 mΩ	0.12	49
C_f	40 mF	0.13	21.9
$C_s + R_s$	0.2 F + 25 mΩ	1.25	217.7
R_{fp}^*	33 mΩ	--	--
Grand Total		93.0	7364

*Weight and size included in Miscellaneous

APS Part Values, Size, and Losses: Table I provides part values for critical components allowing for size and losses of the APS to be calculated. Table I also summarizes the volume and weight required for the APS components. Weight savings provided by the APS are estimated to be more than a factor of 3 if comparing to the use of a conventional passive filter, the brute-force method. Table II provides a summary of predicted component losses.

The MOSFETs used in the implementation of the BDCS are silicon carbide devices. Silicon carbide devices are selected because of the inherently low drain to source parasitic

This article has been accepted for publication in a future issue of this journal, but has not been fully edited. Content may change prior to final publication. Citation information: DOI 10.1109/TPWRD.2015.2478709, IEEE Transactions on Power Delivery

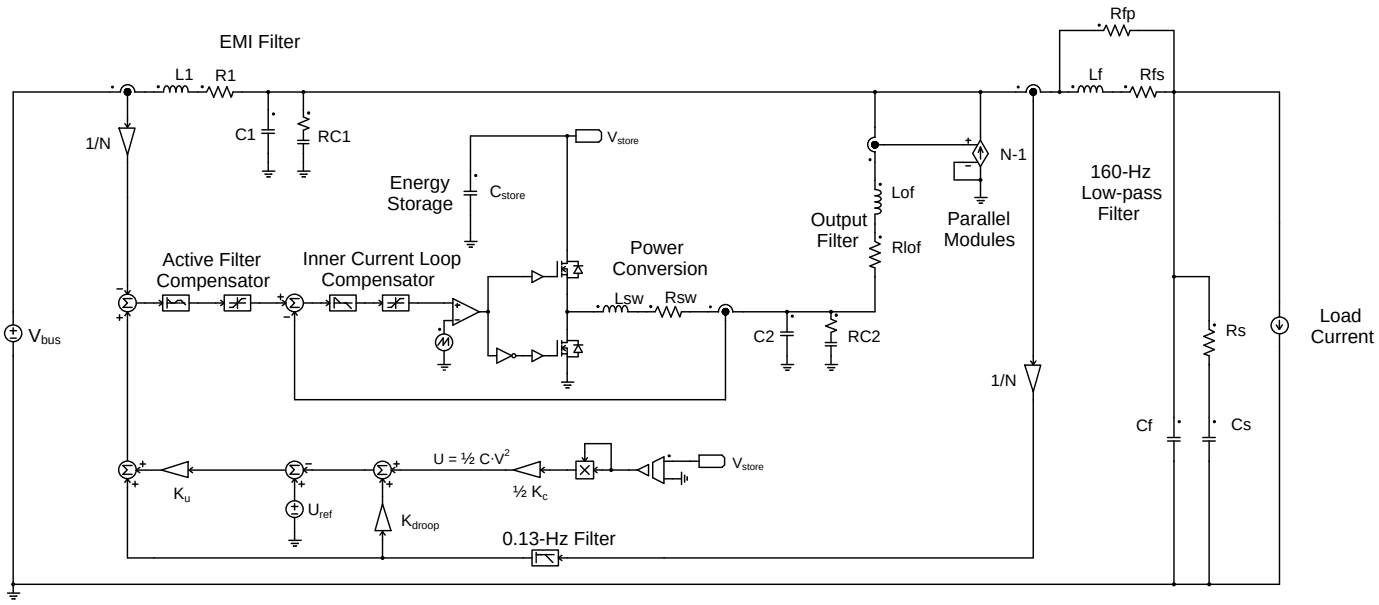

Fig. 6. The high-level schematic of an APS system used for simulation, where N is the total number of parallel modules (N=38).

capacitance, which is crucial to minimizing the switching losses when operating at the high voltage levels with hard switching. The MOSFET part number selected for the low-side switching transistor is the Cree C2M0080120D, whereas the high-side switching transistor is the Cree CMF20120D. The technique defined in Fairchild Semiconductor's AN-6005 application note [19] is used to calculate the losses in the silicon carbide FETs used in the BDCS design.

The magnetic material used for sizing the inductors and calculating the inductor losses is nanocrystalline Vitroperm 500F from Vacuumschmeize. This material has significantly smaller AC core losses with higher saturation flux density capability than other core materials such as MPP, High-Flux, and ferrites. Both of these improved characteristics result in fewer turns needed, and subsequently lower winding loss. Using this material will give smaller and more efficient inductors [20]. By design, the peak flux density for each inductor is limited to less than 0.8 T. The winding fill factor for the inductors has been intentionally made low to achieve the inductance value desired with only a single winding layer. This minimizes the AC winding losses for the 100-μH switching inductor and minimizes winding capacitance for all the inductors.

AC core losses and AC winding losses for the low-pass filter, the output filter, and the EMI filter can be neglected because the AC component of the current and flux density for these inductors is a small value and/or the frequency-spectrum content is very low. The losses for these inductors are dominated by the copper losses determined by the winding resistance and RMS inductor current. But for the 100-μH switching inductor, the AC core losses are the dominant component. The ripple current in the 100-μH inductor is 20 Amps peak-to-peak. This sets the AC flux density level and, knowing the frequency of operation to be 100 kHz, the core loss per unit mass can be determined from the manufacturer core loss versus AC flux density curves specified for a given frequency. Then, knowing the mass of the chosen core, the core loss can be determined. AC winding losses due to the skin effect are small but have been included in the switching-inductor power-dissipation calculation. Winding losses due to the proximity effect are negligible since the winding is on a single layer.

The inductors for the EMI and low-pass filter are the same design. When the APS is active and sinking or sourcing maximum current, only one of these two filters is dissipating power. If the APS is not active, then both the EMI and low-pass filter will be dissipating power, while the APS power dissipation will be negligible. The efficiency number is calculated for the worst case power dissipation condition with the APS active and either the EMI or the low-pass filter dissipating power.

The energy storage capacitor consists of 34 parallel strings of two 5.1-mF capacitors in series, resulting in 86.7 mF per module. Each capacitor is rated for 550 V. In order to achieve the necessary voltage rating, two are placed in series. The capacitors selected are the 500C series type from Cornell Dubilier. The loss due to the energy storage's leakage current and the corresponding current due to the balance resistor across each capacitor is based on a total current draw of 100 μA per capacitor string. To ensure steady-state voltage balance across the capacitors in series, the balance-resistor current is made many times larger than the leakage-current value.

The power dissipation in the low-pass filter damping resistor, R_{fp}, is determined by the current division between the winding resistance of L_f and R_{fp}. Since the winding resistance is much smaller than R_{fp}, negligible power is dissipated in this resistor.

The total system peak losses are estimated to be approximately 6.6 kW under maximum output conditions, giving an efficiency of 97.9%, indicating the potential for significant power savings over the conventional throw-away-power method. To account for various cable losses, connection losses,

This article has been accepted for publication in a future issue of this journal, but has not been fully edited. Content may change prior to final publication. Citation information: DOI 10.1109/TPWRD.2015.2478709, IEEE Transactions on Power Delivery

TABLE II
POWER LOSSES OF THE APS SYSTEM

Single Module Losses		
Max FET (two Cree SiC FETs)	91.9	W
Switching Inductor	32.0	W
Output Filter Inductor	0.5	W
C_{store} Leakage and Balance Resistors	2.6	W
Total Module Losses	127.0	W
Number of Modules	38	
Total BDCS Converter Losses	4826	W
Other Losses		
EMI or Low Pass Filter	210	W
Low Pass Filter Damping	2	W
Miscellaneous & Margin	1512	W
Total System Losses	6550	W

and logic circuitry power dissipation, this number also includes an additional 30% losses captured under the Miscellaneous & Margin heading in Table II.

D. Simulation Results for Notional System

The generator model used in the simulation is based on Simulink's Synchronous Machine standard sixth-order electrical model and is rated for 2.28 MVA. The AVR (voltage) control loop is set at 0.6 Hz and the governor (speed) control loop is set at 1 Hz. The AC/DC converter is an 18-pulse diode rectifier model with an output filter corner frequency of approximately 20 Hz. The major models used to create the AC/DC converter are the three phase-shifting transformers and the 6-pulse diode rectifiers, both from Simulink's SimPowerSystems toolbox [21]. The DC/DC converter voltage control loop is set at 100 Hz. The DC/DC converter is modeled using the standard non-switching average model, which uses an ideal transformer for transforming DC and AC information with the transformer turns ratio controlled by the converter duty cycle [17]. This same technique is used to model the APS bi-directional current source.

To demonstrate the effectiveness and benefits of the APS, Figures 7(a) and 7(b) provide simulation results for various waveforms in the system when a dynamic load is applied both with and without use of the APS. For this simulation, the generator is biased with a 0.6 p.u. load prior to applying the dynamic load.

The load profile chosen in Figures 7(a) and 7(b) not only contains varying duty cycles but also simulates the extreme stressing condition of having significant off times in the load profile, simulating a bang-ON–bang-OFF operation of the 300 kW load, the most stressing condition for the genset. Note that for this extreme profile, the ramp rate seen by the generator with the use of the APS is extremely slow, with the maximum ramp rate shown in 7(b) being less than 0.1 MVA/sec (where 1 p.u. (per unit) is equal to 2.28 MVA). The generator control loops can easily maintain regulation through this very slow changing disturbance. The results also demonstrate that the AC/DC and DC/DC converters do little to reduce the low to medium frequency content, with most of

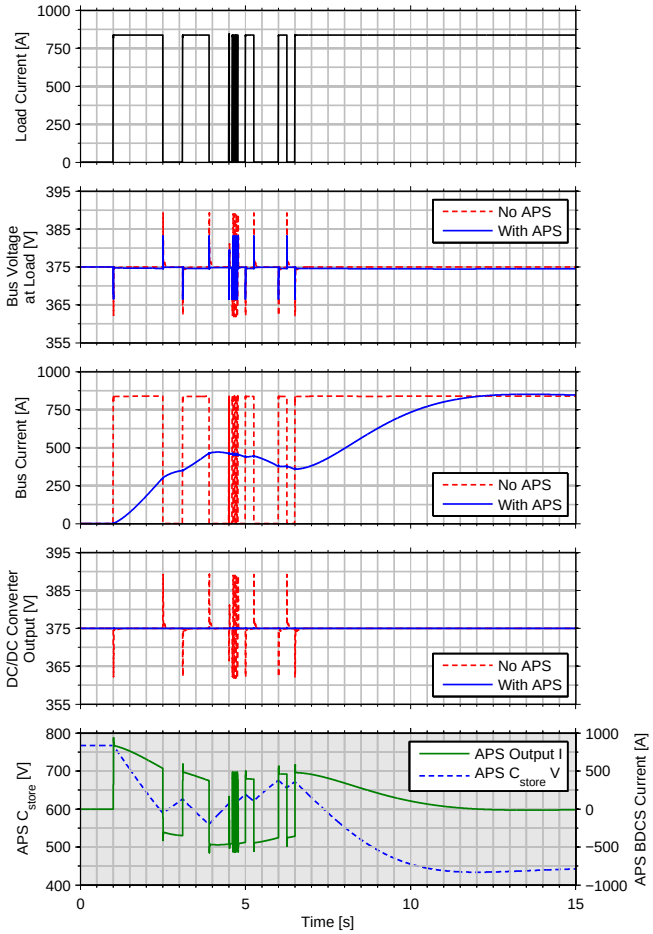

(a) Load and APS results.

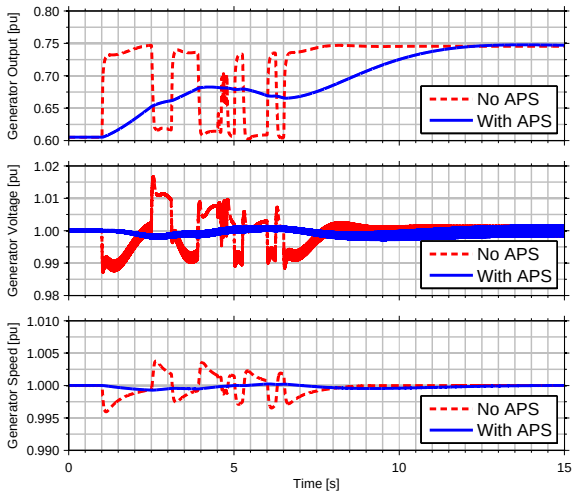

(b) Generator results.

Fig. 7. Simulation results of the first load profile.

This article has been accepted for publication in a future issue of this journal, but has not been fully edited. Content may change prior to final publication. Citation information: DOI 10.1109/TPWRD.2015.2478709, IEEE Transactions on Power Delivery

the dynamic load appearing at the generator terminals when the APS is not used.

As expected, the generator's voltage and prime-mover's speed (frequency) disturbances are much smaller with the use of the APS. The frequency and voltage modulation created by the load without the APS demonstrates that a nominal system of this size encroaches on the respective modulation limits of 0.5% and 2% set by MIL-STD-1399-680 [14]. A larger load or this load combined with other ship loads could result in a noncompliant system.

The genset model used does not simulate mechanical behaviors of the generator, such as shaft or other mechanical resonances. However if shaft resonances are excited (e.g., subsynchronous resonances), significant torques larger than the full-load steady-state torque could be seen on the shaft [6]. Furthermore, if these disturbances exist, mechanical stresses to other parts of the genset can also occur. As is evident in the results, the APS significantly reduces frequencies that could excite potentially dangerous mechanical resonances as well as cause fatigue due to excessive movements.

Figure 7(a) also shows the voltage waveform of the storage capacitor and the current waveform of the bi-directional current source, demonstrating the APS's capability of providing the dynamic demand of the load resulting in the generator only having to provide the rolling average of the load power profile. The 375-V bus voltage delivered to the load is also shown in Figure 7(a), indicating that the $\pm 5\%$ transient regulation requirement is met.

At time 6.5 seconds in Figure 7(a), the load switches to a constant load and the APS consumes no power (APS output current goes to zero) after about 5 seconds from this point in time, demonstrating the efficient conditioning method provided by the APS. If the APS is used for a periodic dynamic load application, the generator will see essentially a constant load with only a benign very small power ripple riding on top of the load's average power draw.

Figure 5 demonstrates the filtering capability of the APS in the frequency domain. The solid blue line in this figure shows the load rejection provided by the APS as viewed from the output of the upstream 375-V converter. The proposed filtering requirement (dashed red line with the 100% and the 3% limits annotated) has been superimposed on the APS results, showing that the APS satisfies the requirement. As can be seen from Figure 5, the APS removes the low to mid frequencies that can degrade the generator shaft or could excite potentially hazardous resonances. In addition, removing these frequencies from the electric plant distribution bus means the bus quality for other users is improved – meaning fewer disturbances will exist due to the load dynamics interacting with the bus impedances and the generator.

IV. Conclusion

The Adaptive Power System (APS) concept presented in this paper can be an enabling technology for sensors or weapons with large dynamic loads, which without the APS would be incompatible with the upstream shipboard generator and distribution bus. The APS consists of energy storage, a bi-directional current source, and innovative control techniques. These innovative control techniques increase the energy storage utilization, thus minimizing the energy storage size. In addition, because of the linear behavior of the outer-energy-loop regulation technique, performance is maintained over all operating conditions. The APS shapes the dynamics seen by the generator to be slower than the response times of the prime-mover's speed or generator's voltage regulation loops, thus allowing the genset to maintain speed and voltage regulation during these large load dynamics. Not only can the APS help to maintain generator/prime-mover reliability, but the APS can also be used to improve sensor/weapon performance or improve metrics such as system weight, cooling demands, and ship fueling costs. Performance of the APS has been demonstrated through the use of Matlab Simulink simulations. Calculated losses and size of a 300-kW system have also been provided, demonstrating that the APS is a viable solution for integrating high-energy sensors and weapons onto Navy platforms.

Acknowledgment

The authors would like to thank JHU/APL's Air and Missile Defense IRAD committee for funding and supporting this work.

References

[1] F. Kanellos, I. Hatzilau, and J. Prousalidis, "Investigation of voltage/frequency modulation in ship electric networks with pulsed loads according to stanag 1008 design constraints," in *All Electric Ship Conference*, 2007.

[2] *IEEE Recommended Practices and Requirements for Harmonic Control in Electrical Power Systems*, IEEE Industry Applications Society/Power Engineering Society Std. 519-1992, 1993.

[3] M. Baldwin, "Electric arc furnace impact on generator torque," in *Power Systems Conference and Exposition, 2004. IEEE PES*, 2004, pp. 776–780 vol.2.

[4] G. J. Tsekouras, F. D. Kanellos, J. M. Prousalidis, and I. K. Hatzilau, "Stanag 1008 design constraints for pulsed loads in the frame of the all electric ship concept," *Nausivios Chora*, vol. 3, pp. 113–152, 2010. [Online]. Available: http://nausivios.snd.edu.gr/nausivios/docs/b3_2010.pdf

[5] H. Smolleck, S. Ranade, N. R. Prasad, and R. Velasco, "Effects of pulsed-power loads upon an electric power grid," *Power Delivery, IEEE Transactions on*, vol. 6, no. 4, pp. 1629–1640, Oct 1991.

[6] D. N. Walker, S. L. Adams, and R. J. Placek, "Torsional vibration and fatigue of turbine-generator shafts," *Power Apparatus and Systems, IEEE Transactions on*, vol. PAS-100, no. 11, pp. 4373–4380, 1981.

[7] M. Butler, G. Dakermanji, L. Goliaszewski, D. Kusnierkiewicz, J. Tarr, D. Temkin, and U. Carlsson, "Fault tolerant shunt regulator for a spacecraft thermionic nuclear reactor," *AIP Conference Proceedings*, vol. 324, no. 1, pp. 39–44, 1995. [Online]. Available: http://scitation.aip.org/content/aip/proceeding/aipcp/10.1063/1.47196

[8] M. Doyle, D. Samuel, T. Conway, and R. Klimowski, "Electromagnetic aircraft launch system-emals," *Magnetics, IEEE Transactions on*, vol. 31, no. 1, pp. 528–533, Jan 1995.

[9] J. Bernardes, M. Stumborg, and T. Jean, "Analysis of a capacitor-based pulsed-power system for driving long-range electromagnetic guns," *Magnetics, IEEE Transactions on*, vol. 39, no. 1, pp. 486–490, Jan 2003.

[10] B. Singh, K. Al-Haddad, and A. Chandra, "A review of active filters for power quality improvement," *Industrial Electronics, IEEE Transactions on*, vol. 46, no. 5, pp. 960–971, Oct 1999.

[11] H. Akagi, "New trends in active filters for power conditioning," *Industry Applications, IEEE Transactions on*, vol. 32, no. 6, pp. 1312–1322, Nov 1996.

[12] ——, "Active harmonic filters," *Proceedings of the IEEE*, vol. 93, no. 12, pp. 2128–2141, Dec 2005.

[13] D. Hamza and P. Jain, "Conducted emi noise mitigation in dc-dc converters using active filtering method," in *Power Electronics Specialists Conference, 2008. PESC 2008. IEEE*, June 2008, pp. 188–194.

[14] *High Voltage Electric Power, Alternating Current*, Department of the Navy Std. MIL-STD-1399-680, 2008.
[15] *Governing Systems, Speed & Load-Sensing Naval Shipboard Use*, Department of the Navy Std. MIL-G-21 410A, 1991.
[16] *Regulator-Exciter Systems, Voltage, A.C. Generator, Naval Shipboard Use*, Department of the Navy Std. MIL-R-2729D, 1992.
[17] N. Mohan, *Power electronics : a first course*. Hoboken, N.J: Wiley, 2012.
[18] R. Dorf, *Modern control systems*. Upper Saddle River, N.J: Pearson Prentice Hall, 2011.
[19] J. Klein, "Synchronous buck mosfet loss calculations with excel model," *Fairchild Semiconductor*, no. AN-6005, November 2014.
[20] L. Kvarnsjö, "Green inductive components," *Special Report – Green Power*, 2009.
[21] MATLAB & SIMULINK, *SimPowerSystems™ User's Guide 5.8 (R2013a)*. The MathWorks, Inc., 2013.

Deanna Temkin is a member of the principle professional staff at the Johns Hopkins University Applied Physics Laboratory in the Radar and EW Systems Development Group. Her current work is aimed at addressing power system challenges and requirements as related to integrating sensors and weapons onto Navy platforms. Ms. Temkin's previous work includes hardware design and development of spacecraft power systems and power converters. She received her B.S. degree from the University of Virginia and her M.S. degree from the University of Maryland, both in electrical engineering.

Tyler Boehmer currently works for the Johns Hopkins University Applied Physics Laboratory in the Radar and EW Systems Development Group, focusing on shipboard integration of large sensors for the Navy. He received his B.S. and M.S. degrees in electrical engineering from the Pennsylvania State University. Mr. Boehmer's current research interests include shipboard power systems and high-power converters.

Amy Billups is a member of the principle professional staff at the Johns Hopkins University Applied Physics Laboratory in the Radar and EW Systems Development Group. She has 16 years experience in mechanical design and ship integration of radar systems. Ms. Billups received her B.S. and M.S. degrees in mechanical engineering from West Virginia University, a M.S. degree in electrical engineering from Johns Hopkins University and is currently pursuing a PhD in mechanical engineering from the University of Maryland.